Journal of Bio- and Tribo-Corrosion (2023) 9:61
https://doi.org/10.1007/s40735-023-00776-3

Combination of Experimental and Computational Insight into the Anti-corrosion Performance of 1-(4-tert-butylphenyl)-4-(4 -(benzhydryloxy)piperidin-1-yl)butan-1-one onto C-steel in Acidic Environments

Salah Eid[1,2] · Kamal A. Soliman[2] · A. Y. El-Etre[2] · Ehab Gad[1,3] · H. Nady[1,4]

Received: 22 January 2023 / Revised: 12 April 2023 / Accepted: 20 June 2023 / Published online: 4 July 2023

Abstract

Metals are shielded from corrosion damage using a variety of techniques, including the use of inhibitors. 1-(4-tert-butylphenyl)-4-(4-(benzhydryloxy)piperidin-1-yl)butan-1-one (known as *Ebastine* drug) was evaluated as a novel inhibitor for corrosion of C-steel in HCl (1.0 M) solution. Utilizing weight loss (WL) and potentiodynamic polarization (PDP) approaches, the inhibitory performance of the Ebastine molecule was investigated. The inhibition efficacy became observed to rise with incrementing of the *Ebastine* concentration and diminish with growing temperature. The amounts of activation energy (E_a) and heat of adsorption (Q_{ads}) were enumerated and elucidated. The concept of the adsorption of *Ebastine* molecules on the surface of C-steel was used to explain the inhibitory behavior, which constitutes obstruction of charge and mass transfer give rise to guard the C-steel against the offensive ions. Also, the surface morphology of C-steel immersed in HCl (1.0 M) solution in the lack and existence of the *Ebastine* molecule was examined by SEM and AFM. Finally, density functional theory (DFT) was employed to examine the *Ebastine* molecule. The mechanism through which Ebastine is adsorbed to the surface of Fe (110), was estimated by Monte Carlo (MC) simulation.

✉ Salah Eid
salaheed@ju.edu.sa

[1] Chemistry Department, College of Science and Arts, Jouf University, Alqurayat, Saudi Arabia

[2] Chemistry Department, Faculty of Science, Benha University, Benha, Egypt

[3] Chemistry Department, Faculty of Science, Al-Azhar University, Nasr City, Egypt

[4] Chemistry Department, Faculty of Science, Fayoum University, Fayoum, Egypt

Graphical Abstract

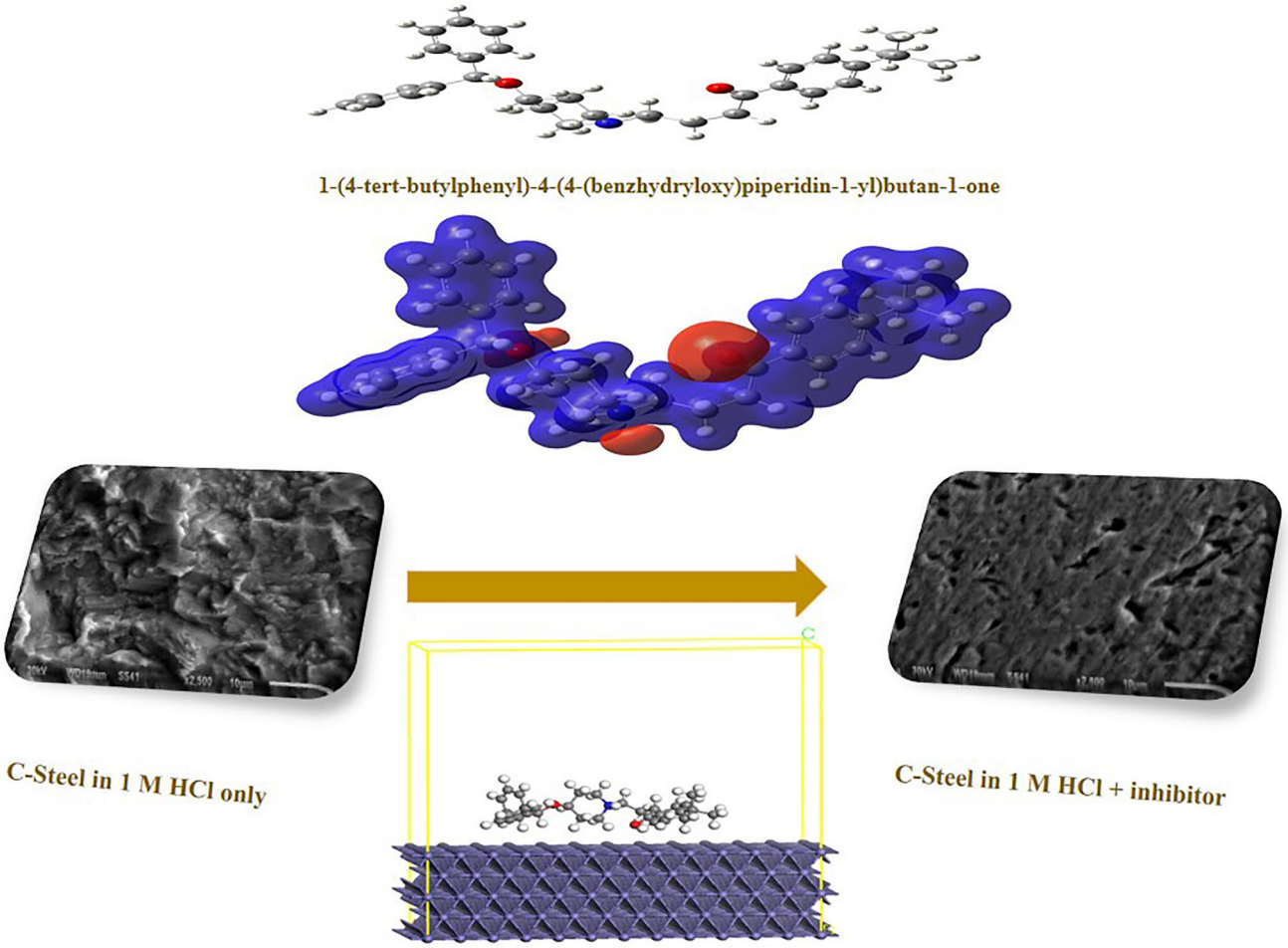

Keywords Drug · Ebastine · C-steel · Corrosion inhibitor · DFT

1 Introduction

C-steel is utmost commonly appropriated as the basic structural material in a variety of fields due to its superior mechanical and economic advantages, including chemical processing, maritime applications, the oil and gas industry, and purifying equipment [1, 2]. In plentiful applications, it suffers from corrosion that reason thousands of millions of USD lost [2, 3]. Acidic media, substantial solutions of HCl acid, are broadly exercised in chemical and high-quality industrial techniques together with acid pickling, acid descaling, acid cleaning, and oil wet cleansing of metals and their alloys [4–8]. Different methods are applied to decrease the rate of corrosion, like utilizing inhibitors [9, 10]. Plentiful surveys had been achieved on reduce C-steel corrosion in acidic media [11–14].

It is well known that organic molecules can effectively suppress corrosion, particularly those that contain heteroatoms like nitrogen, sulfur, and oxygen [15]. The ability of these chemical inhibitors to bind to the metallic surface is correlated with their efficacy [16]. It is appreciated that with organic heterocyclic compounds, the coordinate

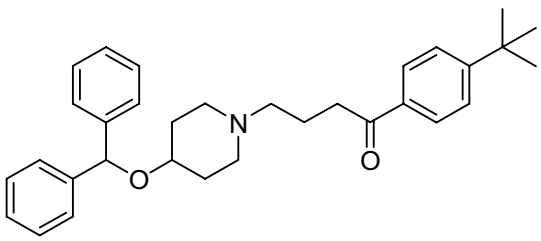

Fig. 1 The chemical structure of *Ebastine*

links are stronger and exhibit high inhibition efficiencies. Following a number of research concerning, it has been determined that the attitude of the corrosion inhibitor is connected to the inhibitor's molecular structure, molecular electronic distribution, surface charge occupation, and attraction to metal surfaces [17]. So varied structures have been created to value their corrosion inhibition abilities [18]. Utilized inhibitors can also have some hazards because it's far hurtful to humans and surroundings and expensive. It may overcome these flaws by utilizing expired drugs. Several pharmaceuticals are returned to their manufacturers since they will expire, causing economic losses to the manufacturers. A wealth of substances found in the returned (or expired) drugs can sometimes be recycled and utilized for diverse purposes, like corrosion prevention [19–28]. The aim of this paper is to look at the inhibiting behavior of 1-(4-tert-butylphenyl)-4-(4-(benzhydryloxy)piperidin-1-yl)butan-1-one, known as *Ebastine* drug, on the corrosion of C-steel X52 in HCl (1.0 M) solution. In the investigation, potentiodynamic polarization (PDP), weight loss (WL), SEM and AFM methods have been used. Additionally, the activation energy (E_a) and heat of adsorption (Q_{ads}) were estimated and described. In order to comprehend the corrosion inhibition mechanism, DFT and MC simulation were also utilized to investigate the *Ebastine*.

2 Experimental

2.1 Test Solutions

All the tested solutions have been prepared to utilize analytical-grade chemical substances and distilled water. The 1-(4-tert-butylphenyl)-4-(4-(benzhydryloxy)piperidin-1-yl) butan-1-one, known as *Ebastine*, was gained from a medication called evastine that was made in Egypt by the Marcyrl Company. The medicine contains 5 mg of *Ebastine* per 5 ml. The volume needed to achieve the desired concentration was determined then created through dilution. *Ebastine* has a molar mass of 469.658 g/mol and the chemical formula $C_{32}H_{39}NO_2$. Figure 1 depicts the *Ebastine* structure.

2.2 Weight Loss (WL) Experiments

The WL tests had been carried out utilizing C-steel X52 (CSX52) specimens which have the following composition: 0.28% C, 1.4% Mn, 0.03% S, 0.03% P, ≤ 0.06% Np, ≤ 0.06% V ≤ 0.06% Ti, and residuum iron. The pieces of CSX52 were utilized for WL measurements with dimensions (1.4 × 1.2 × 4 cm). The CSX52 coupons were cleaned with distilled water, CH_3COCH_3 and then distilled water once more after being polished with various emery paper grades. The pieces were correctly weighted and subsequently sunken in HCl (1.0 M) solution lack and existence specific *Ebastine* concentrations at a temperature of 30 °C. The temperature for weight reduction tests became controlled by employing a water bath furnished with thermostat control ± 1 °C. After 24 h exposure, the tested pieces have been removed, rinsed very well with distilled water, desiccated, and meticulously weighed. In this research, all evaluations were conducted in a naturally aerated environment [1]. To achieve reproducibility, each experiment was carried out at least twice.

2.3 Potentiodynamic Polarization Measurements (PDP)

The running electrode had an exposed surface area of 2.24 cm^2 and was made from CSX52 implanted in epoxy holders. Before being applied, the electrode has been polished with diverse emery paper grades up to 2500 grade, degreased with CH_3COCH_3, then cleaned with distilled H_2O. As counter and reference electrodes, a Pt sheet and a calomel electrode were used, respectively. Using a PS potentiostat and PS6 software, PDP tests were completed [4, 29] at a scan rate of 1.0 mV/sec. To achieve reproducibility, each experiment was carried out at least twice.

2.4 SEM Measurements

After being abraded with diverse emery papers up to a 2500 grade, the C-steel X52 coupons were maintained for 24 h in HCl (1.0 M) with and without 17.03×10^{-5} M of *Ebastine*. The samples were then dried, desiccated, and placed into the spectrometer after being cleaned with distilled water. At Egypt's Mansoura University, the SEM observation is carried out with the JSM-6510LV.

2.5 Computational Details

DFT calculations employing the B3LYP functional [29] and the 6–31 g (d, p) basis set implemented in the Gaussian 09 program [30] were used to thoroughly optimize the *Ebastine* molecule. In the gas phase, the computations were carried out. The simulation findings include the following: the highest occupied molecular orbital (HOMO), dipole moment (μ), hardness (η), energy gap (ΔE), and the lowest unoccupied molecular orbital (LUMO), the number of electrons transferred (ΔN), and global softness (σ) were investigated. The global softness, hardness and the number of electrons transferred were calculated as follows:

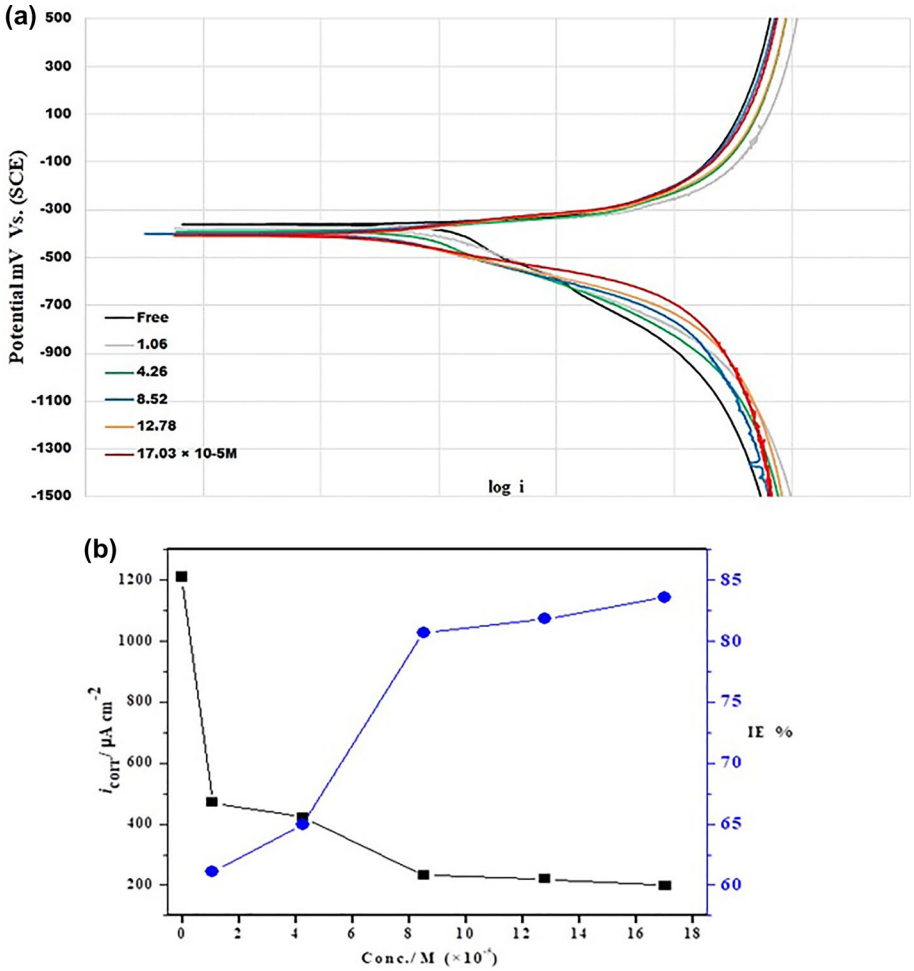

Fig. 2 **a** Potentiodynamic polarization graphs of CSX52 electrode in (1.0 M) HCl solution containing different amounts of *Ebastine*, **b** the effect of increasing concentration of *Ebastine* on the current density and the inhibition efficiency

Table 1 Corrosion parameters of CSX52 electrode in HCl (1.0 M) solutions free and containing diverse concentrations of *Ebastine* at 303 K

Conc $\times 10^{-5}$ M	β_a mV decade^{-1}	$\beta -_c$ mV decade^{-1}	E_{corr} mV, SCE	i_{corr} µA cm^{-2}	%IE	θ
0.00	41	267	− 367	1210	–	–
1.06	27	154	− 367	471	61.1	0.611
4.26	36	202	− 377	423	65.0	0.650
8.52	50	130	− 389	233	80.7	0.807
12.78	54	114	− 398	220	81.8	0.818
17.03	55	90	− 402	198	83.6	0.836

$$\eta = \frac{E_{LUMO} - E_{HOMO}}{2} \quad (1)$$

$$\sigma = \frac{1}{\eta} \quad (2)$$

$$\Delta N = \frac{\phi - \chi_{inh}}{2(\eta_{Fe} + \eta_{inh})} \quad (3)$$

where φ, χ_{inh}, η_{inh}andη_{Fe} are the function work of Fe (110) (4.820 eV), *Ebastine* electronegativity, *Ebastine* chemical hardness and, iron chemical hardness (0 eV *Ebastine*) respectively.

2.6 MC Simulations

For the purpose of this work, a single inhibitor molecule was chosen to be adsorbed to the Fe (110) surface. The adsorption locator module performed the MC

simulation. By constructing a 12 × 12 supercell with a 20 vacuum height above the surface, the surface Fe (110) was improved. Condensed-phase optimized molecular potentials for atomistic simulation studies (COMPASS) were applied to the adsorption process. For electrostatic summation, the Ewald methodology was adopted, and for van der Waals, the atom-based strategy. The following equation was used to compute the inhibitor's adsorption energy:

$$E_{ads} = E_{complex} - E_{Fe} - E_{inh} \quad (4)$$

where $E_{complex}$, E_{inh}, and E_{Fe} are the total energies of inhibitor on Fe (110) surface, the energy of *Ebastine* molecule, and energy of iron(110) surface, respectively.

3 Results and Discussion

3.1 Potentiodynamic Polarization (PDP)

At a scan rate of 0.001 V/sec, the PDP curves of CSX52 in HCl (1.0 M) solutions were shown, Fig. 2, both uninhibited and with varying amounts of *Ebastine*. Table 1 presents the competent electrochemical parameters, including

Table 2 The effect of adding various *Ebastine* concentrations on the weight loss of CSX52 in HCl (1.0 M) solution at 303 K

Inh. Conc $\times 10^{-5}$ M	Weight loss (gm)	% IE	θ
0	0.4774	–	–
1.06	0.0799	83.26	0.8326
4.26	0.056	88.27	0.8827
8.52	0.03160	93.38	0.9338
12.78	0.0252	94.72	0.9472
17.03	0.02	95.81	0.9581

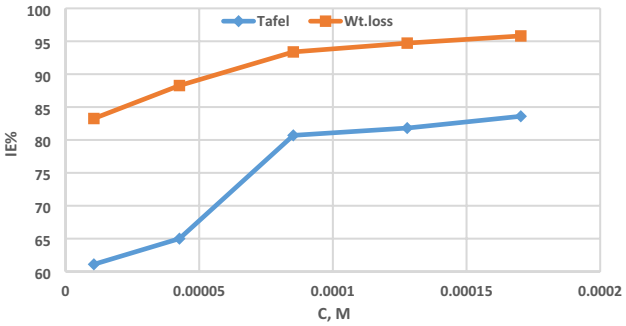

Fig. 3 Relations between (% IE) and *Ebastine* concentration obtained from two different techniques

surface coverage (θ), the percentage of inhibitory efficacy (%IE), anodic and cathodic Tafel slopes (β_a and β_c), corrosion current (i_{corr}), corrosion potential (E_{corr}). In order to calculate the (%IE) and surface coverage (θ), the following equations [31, 32] were used:

$$\%IE = \left(1 - i_{inh}/i_{Free}\right) 100 \quad (5)$$

$$\theta = \%IE \,/\, 100 \quad (6)$$

where i_{Free} and i_{inh} are the (i_{corr}) of the CSX52 electrode in the lack and presence of *Ebastine* drug, respectively.

When the amount of *Ebastine* is increased, Table 1's analysis reveals that the value of (i_{corr}) falls and the inhibition activity rises. This finding demonstrates how the tested *Ebastine* inhibits the breakdown of CSX52 in HCl (1.0 M) solution. In the existence of *Ebastine*, the corrosion potential value is unaffected. Furthermore, the addition of rising *Ebastine* concentrations considerably changed the cathodic tafel constants. These findings lead to some confusion about the kind of metal sites at which the inhibitor molecules adsorb. The former suggests a

Table 3 Comparison of the inhibitory effectiveness of several drug inhibitors used for iron corrosion in various environments

Inhibitor	Conc	Metal	Medium	Measurement method	Inhibition efficiency	References
Tenormin drug	300 ppm	304 stainless steel	2 M HCl	Weight loss	92.2	[20]
				PDP	75.1	
Desloratidine drug	19.3×10^{-5} M	Carbon steel	1 M HCl	Weight loss	92.7	[23]
				PDP	85.2	
Ambroxol drug	9 V/V%	Mild steel	1 M HCl	Weight loss	84.34	[25]
				PDP	59.47	
Spironolactone drug	7.2×10^{-3}	C38 carbon steel	10% HCl	Weight loss	98.1	[28]
				PDP	95.8	
Ebastine drug	17.03×10^{-5}	Carbon steel	1 M HCl	Weight loss	95.8	This work
				PDP	83.6	

mixed adsorption process, while the latter supports the cathodic adsorption mechanism. However, careful investigation of the figure of the Tafel technique reveals that the values of the Tafel constants are the mean criteria that determine the kind of inhibition process. Thus, based on this argument, *Ebastine* is considered to be a cathodic inhibitor. The molecules of cathodic inhibitor resort to being adsorbed on the cathodic sites on the metal rather than the anodic ones [33].

3.2 Weight Loss Studies

After 24 h, the corrosion of CSX52 in HCl (1.0 M) solution was examined for the impacts of rising the amounts of *Ebastine* on WL, (%IE), and the quantity of surface covering (θ), Table 2. Using the formula found in next equation [34], the inhibitory efficacy was determined:

$$\%\mathrm{IE} = \left(1 - W_{\mathrm{Inh}}/W_{\mathrm{Free}}\right) \times 100 \tag{7}$$

where W_{Free} and W_{Inh} are the WL of CSX52 after 24 h in the existence and absence of *Ebastine*, respectively. The WL was discovered to be reduced when *Ebastine* concentrations rise, although surface coverage and inhibitory efficacy increase. The experimental outcomes of this work are compared with past iron corrosion drug inhibitors in various media, as shown in Table 3. The protective layer created by the *Ebastine* appears to have a high anticorrosive capacity than many other iron inhibitors, according to the findings of weight loss and potentiodynamic polarization measurements.

The relations between (%IE) and *Ebastine* concentration as obtained from WL measurements and polarization technique were presented in Fig. 3. The figure shows that the inhibition efficiency values obtained from WL measurements are higher than those obtained from the Tafel technique, this also appears in much other literature, as seen in Table 3, especially at low concentrations. This discrepancy appears may be due to the different nature of the two techniques. However, the general dependence of inhibition efficiency on inhibitor concentration is the same for both. It could be easily seen that a very low concentration is needed to perform high inhibition efficiency. This result could be imputed to horizontal adsorption of the *Ebastine* molecules on the metal surface, covering a large surface area with a small number of them. Moreover, the figure shows that the value of inhibition efficiency then becomes almost independent of the inhibitor concentration. It could be concluded that, as the surface becomes almost saturated with adsorbed molecules, there is no longer an impact of increasing *Ebastine* concentration on the value of inhibition efficacy.

3.3 Morphology Measurements

Studying the morphology of the surface was an excellent gauge of how incisive the corrosion attack was. After being submerged in 1.0 M HCl, in the lack and containing17.03×10^{-5} M of *Ebastine*, CSX52 coupons were seen utilizing SEM, Fig. 4. The morphology, as revealed by SEM results, of CSX52 coupons in HCl (1.0 M) only revealed that the surface is strongly distorted. Otherwise, in HCl (1.0 M) solution containing *Ebastine* [35–37], the surface of CSX52 becomes smoother and less damaged, regardless of the presence of some small pits on the surface. These small pits may be another reason for the difference in the amount of protection efficiency obtained from chemical and electrochemical techniques.

AFM offers surface topography images with atomic or near-atomic resolution that can be used to determine a coupon's surface roughness. Figure 5 displays both the *Ebastine*-free and *Ebastine*-containing *Ebastine*, AFM morphologies for the CSX52 surface in HCl (1.0 M) solutions. According to Fig. 5, the average roughness and the root mean square for CSX52 surface in HCl (1.0 M), 978.76×10^{-9} m and 1234.9×10^{-9} m, have higher values than CSX52 sample in existence of *Ebastine*, 272.8×10^{-9} m and 336.58×10^{-9} m, respectively [23]. These findings demonstrate that *Ebastine* molecules are adsorbed on the CSX52 surface and have created a shielding a protective film that effectively protects the CSX52 surface from the aggressive ions [23].

3.4 Adsorption Isotherm

Finding an appropriate isotherm enables the interpretation of Ebastine's adsorption behavior on the CSX52 surface. To fit the exploratory data of WL measurements, various numerical relations for the adsorption isotherms were proposed [38]. The Freundlich, Langmuir, Frumkin, Temkin, Al Awady and Florry Huggins isotherms [38] were looked into to better understand the mechanism at play in the case of *Ebastine*, Fig. 6. Langmuir isotherm equation [39] fits our results:

$$C/\theta = 1/K + C \tag{8}$$

where K and C stand for the equilibrium constant of the adsorption process and the *Ebastine* concentration, respectively. In Fig. 6, a graph of C/θ Vs. C is shown. The standard free energy of adsorption, $\Delta G^{\mathrm{o}}{}_{\mathrm{ads}}$, is related to the adsorption equilibrium constant, K, by the next equation [34, 39]:

$$K = 1/55.5 \exp\left(-\Delta G^{o}_{\mathrm{ads}}/RT\right) \tag{9}$$

where the number 55.5 denotes the molar concentration of water and the letters T and R stand for the absolute temperature and the ideal gas constant, respectively.

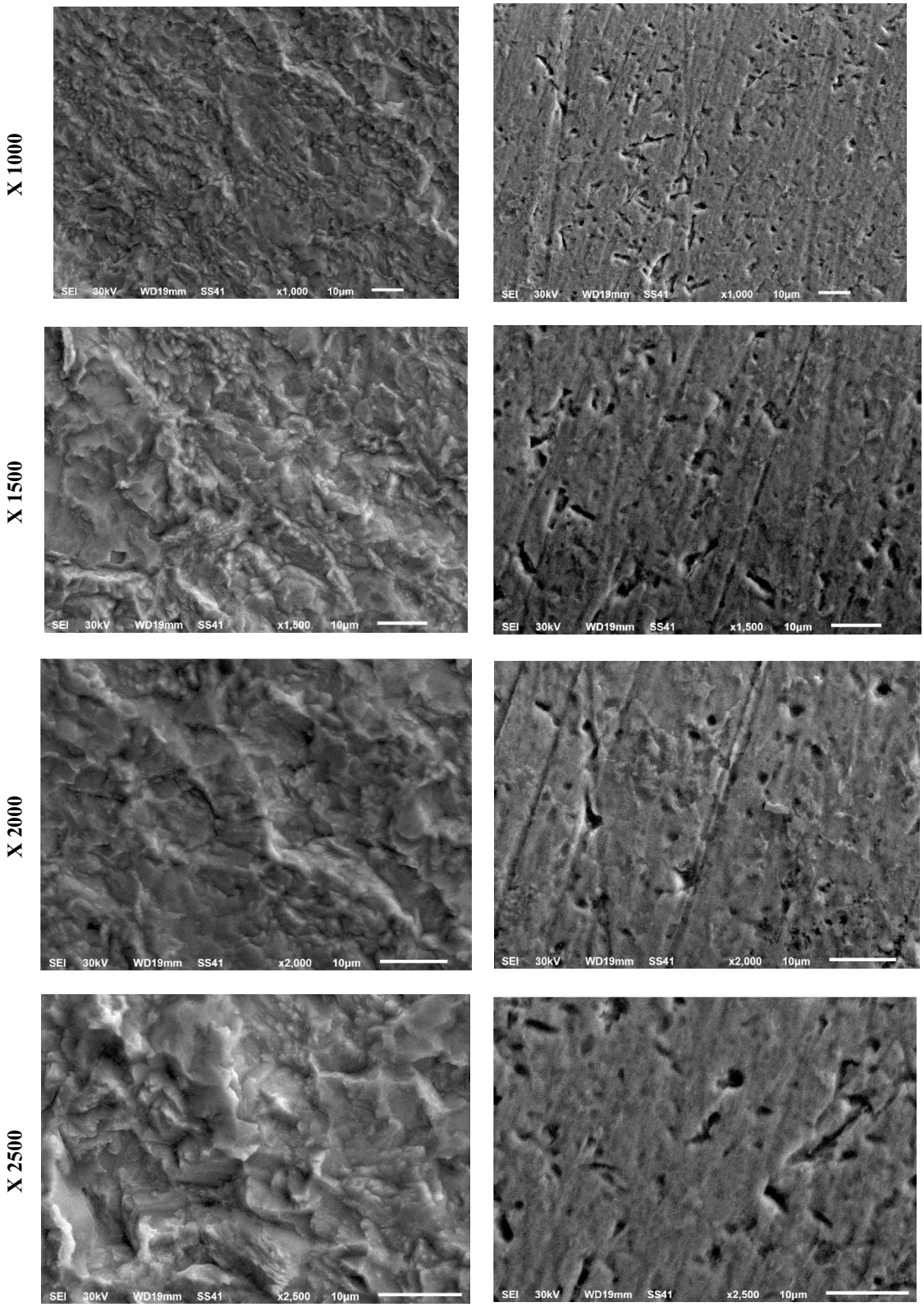

a) SEM after immersion in HCl (1.0 M) **only**

b) SEM after immersion in HCl (1.0 M) **in presence of 17.03 ×10^{-5} M from Ebastine**

Fig. 4 SEM for CSX52 coupons after immersion in HCl (1.0 M) in lack and containing 17.03×10^{-5} M from *Ebastine* drug

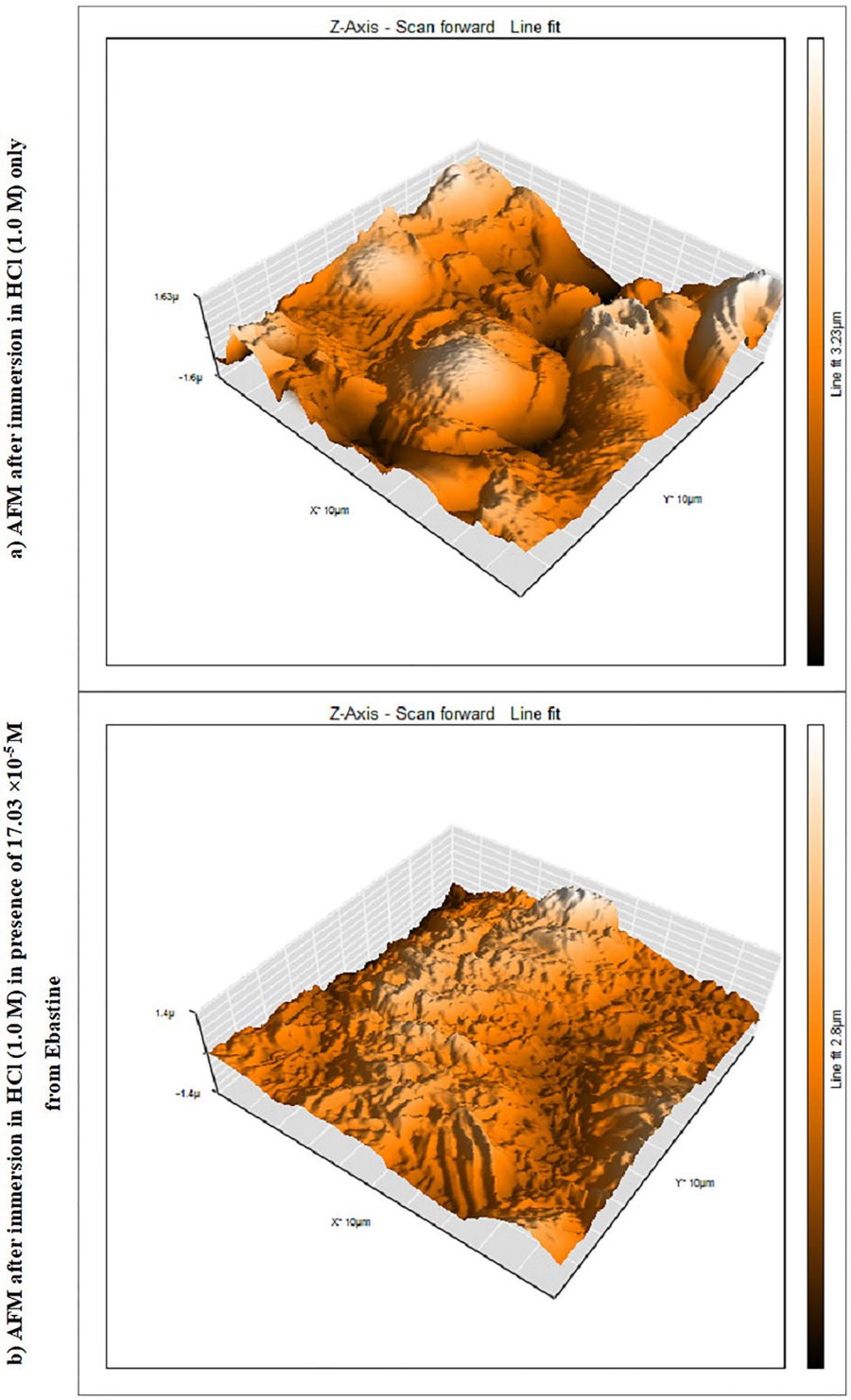

Fig. 5 AFM for CSX52 coupons after immersion in HCl (1.0 M) in free and containing *Ebastine* drug

The equilibrium constant and the standard adsorption-free energy are equal to 33.3×10^4 and − 42.15 kJ mol^{-1}, respectively. The spontaneous nature of *Ebastine's* adsorption process on the CSX52 surface is indicated by the negative sign of ΔG^{o}_{ads}. The obtained value of ΔG^{o}_{ads} suggests a chemical adsorption process [34, 40].

3.5 Thermodynamic/Adsorption Calculations

The effect of temperature rise on the WL and corrosion rate of CSX52 in HCl (1.0 M) in the existence and absent of 17.03×10^{-5} M *Ebastine* are shown in Table 4 after a 24 h period. According to the research, *Ebastine* works well as an inhibitor at high temperatures, and the effectiveness of

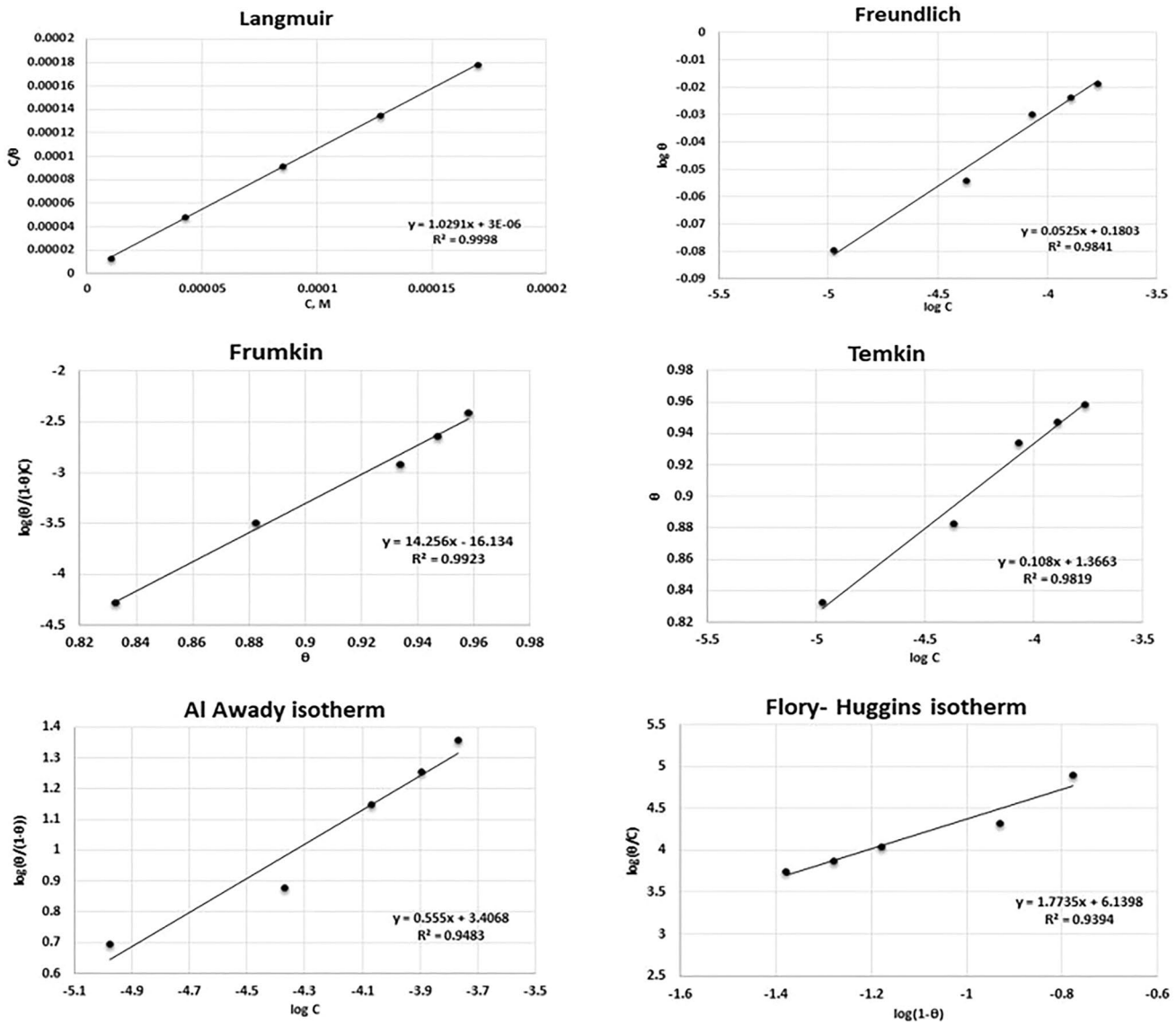

Fig. 6 Isotherms for the *Ebastine* compound adsorbed on the CSX52 surface in HCl (1.0 M)

Table 4 The adsorption parameters values of CSX52 in HCl (1.0 M) with 17.03×10^{-5} M *Ebastine*

Solution	wt_1 30 °C	wt_2 50 °C	r_1 303 K $10^{-3} \times$g cm^{-2} d^{-1}	r_2 323 K $10^{-3} \times$g cm^{-2} d^{-1}	θ_1 30 °C	θ_2 50 °C	E_a $10^2 \times$J mol^{-1}	$-Q_{ads}$ kJ mol^{-1}
Free	0.4774	1.1145	19.76	46.13	–	–	345	–
Ebastine	0.02	0.3648	0.828	15.10	0.9581	0.6726	1182	98.05

inhibition declines as temperature increases. This suggests that the adsorption took place via a physical mechanism [34, 41]. The apparent activation energy, E_a, for CSX52 corrosion in HCl (1.0 M) in the lack and existence of 17.03×10^{-5} M *Ebastine* was calculated utilizing the Arrhenius type equation [23, 42]:

$$\log\left(r_2/r_1\right) = \left(E_a/2.303R\right)\left(\left(1/T_1\right) - \left(1/T_2\right)\right) \quad (10)$$

where T is the absolute temperature, E_a is the apparent activation energy, R is the universal gas constant, A is the Arrhenius pre-exponential factor, and r_1 and r_2 are the corrosion rates derived at temperatures T_1 and T_2, respectively, after 24 h. The activation energy (E_a) values are listed in

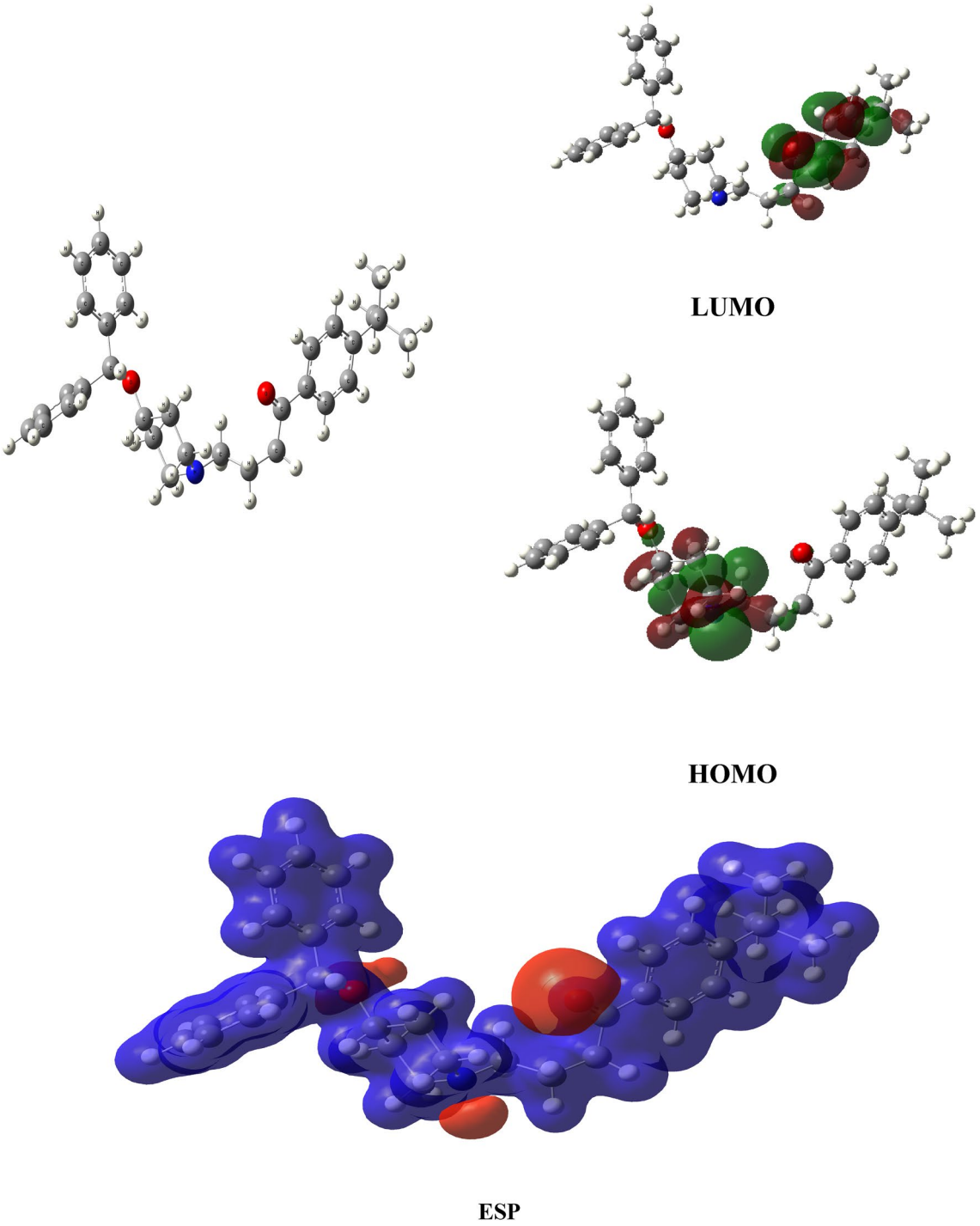

Fig. 7 The optimized structure, frontier molecular orbitals (HOMO and LUMO) and ESP for of *Ebastine*

Table 5 Quantum chemical descriptors of *Ebastine*

Quantum descriptor	HOMO (eV)	LUMO (eV)	ΔE (eV)	Dipole moment (Debye)	η (eV)	σ (eV^{-1})	ΔN (e)
	− 5.35	− 1.42	3.93	3.13	1.97	0.51	0.36

Table (4). The data show that the addition of the *Ebastine* results in an increase in the apparent activation energy value. This outcome confirms the physical adsorption process [23, 41].

The heat of adsorption of the *Ebastine* was computed utilizing the next equation [34]:

$$Q_{ads} = 2.303\,R\,[\log(\theta_2/(1-\theta_2)) - \log(\theta_1/(1-\theta_1))] \times [T_1T_2/(T_2 - T_1)] \quad (11)$$

where θ_1 and θ_2 are the fractions of surface coverage at temperatures T_1 and T_2, respectively. Table 4 displays the value of Q_{ads} after it has been calculated. The fact that Q_{ads} is negative indicates that the drug, *Ebastine*, under study is being adsorbed exothermically to the CSX52 surface.

A careful examination of the results reveals consistency regarding the mode of adsorption. While the value of adsorption-free energy suggests a chemical adsorption process, the temperature effect supports a physical adsorption mechanism. Both mechanisms can occur together when the molecules adsorb physically and then form a sort of chemical combination with dissolved metal cations upon arriving at the double-layer vicinity. If the formed compound is unstable, it will be decomposed by rising temperatures.

3.6 DFT Calculations

The optimized *Ebastine* structure at the B3LYP level of theory is shown in Fig. 7, together with their frontier molecular orbitals. With a higher HOMO energy value, which indicates a greater electron donation of the *Ebastine* molecule to the steel's empty d-orbital, and a lower LUMO energy level, which indicates the ability of the *Ebastine* to gain electrons from the steel's d-orbital, the binding of *Ebastine* molecules to the C-steel interface increases. [42]. *Ebastine* has a high HOMO and a low LUMO energy value, as seen in Table 5, indicating that it has a strong inhibitory efficiency. The inhibitor's adsorption capacity improves as the energy gap narrows. The effectiveness of inhibition and chemical reactivity improves with diminishing energy gaps [43, 44]. Table 5 shows that *Ebastine* has a small energy gap.

HOMO electron distribution for the *Ebastine* as seen in Fig. 7, was localized on the piperidyl moiety, while LUMO electron density was distributed on benzoyl moiety. An essential quantum descriptor that captures the overall polarity of a molecule is the dipole moment (μ). The μ is associated with inhibition efficacy. The inhibition efficacy rises with the increment of the μ. The *Ebastine* has a strong dipole moment, as indicated in Table 5.

Additionally, the electrons transferred number (ΔN) is meant. When ΔN values $<$ 3.6, the protective efficiency increases by incrementing the ability of the *Ebastine* molecule to contribute electrons to CSX52 surface [45, 46]. As demonstrated in Table 5, the ΔN value for *Ebastine* is positive, indicating that the *Ebastine* inhibitor has high inhibitory efficiency.

Table 5 shows the global softness (σ) and hardness (σ) of the *Ebastine* inhibitor, which affect the reactivity of the *Ebastine* molecule. The *Ebastine* has a high softness value and a low hardness value, indicating a strong inhibitory efficiency.

The *Ebastine* molecule's reactive locations are identified using a visual tool called the molecular electrostatic potential map (ESP). The red and yellow areas represent negative ESP. The most reactive atoms are those with a higher negative charge. The nitrogen and oxygen atoms of

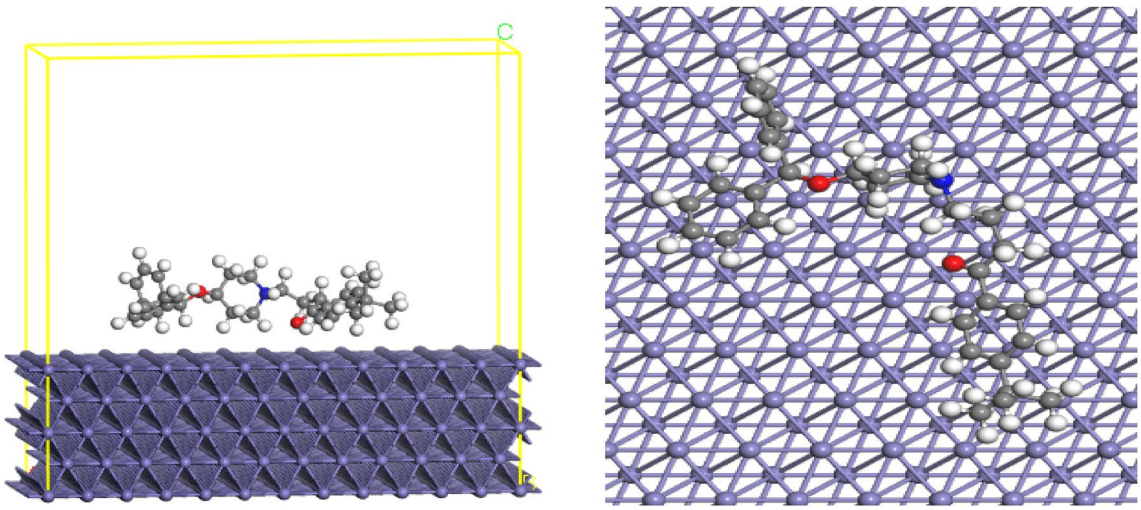

Fig. 8 Adsorption of *Ebastine* on Fe (110) surface top and side view

the investigated inhibitors are where the negative ESP is situated, as can be observed in Fig. 7.

3.7 MC Simulation

MC simulation can be utilized to discover the majority of *Ebastine* molecule configurations that are adsorbed on a CSX52. The *Ebastine* was replicated in both the vacuum and gas phase. According to Fig. 8, *Ebastine* adsorbed on Fe (110) in a parallel configuration. Ebastine's adsorption energy values on Fe (110) were discovered to be − 176.32 kcal/mol. The high adsorption energy of the *Ebastine* causes a strong contact of *Ebastine* inhibitor on Fe (110), resulting in the formation of a protective film on the CSX52 surface from the harsh environment (HCl solution), resulting in enhanced inhibition efficacy.

3.8 Mechanism of Inhibition

The PDP results have suggested a cathodic inhibition mechanism. This mechanism may be explained by the existence of nitrogen and oxygen atoms in the inhibitor's molecule. Due to the existence of lone pairs of electrons at these atoms, protons are attached to them from the acidic solution, forming positive molecules. Thus, the adsorption of these formed positive structures is expected to be selectively adsorbed on the cathodic sites at the surface of the C-steel. Figure 8 represents a schematic drawing that illustrates the adsorption mode of the *Ebastine* molecule. As the *Ebastine* molecules reach the surface of C-steel under the effect of their charges, they form a weak bonding compound with the dissolved metal cations. The formed compound covers the metal surface, leading to the inhibition process. However, increasing temperature decomposes the formed layer, resulting in a lowering in the inhibition efficacy. The results also showed that a very small concentration of the compound is enough to reach the highest possible inhibition efficacy. Increasing the additive concentration beyond this concentration results in a steady increase in the inhibition efficacy. This finding leads to the conclusion that the compound molecules adsorb horizontally on the electrode surface. The adsorbent's horizontal position ensures a larger covered area for each adsorbed molecule. Thus, a smaller number of molecules is needed to reach the maximum attainable efficacy.

4 Conclusions

- *Ebastine* reduces the CSX52 corrosion and its inhibitive effect depends upon its concentration.
- In HCl (1.0 M) solution, *Ebastine* follows the Langmuir isotherm when adsorbing on CSX52 surfaces.
- The adsorption of *Ebastine* on the surface of CSX52 is the cause of the conduct inhibition, which prevents charge and mass transfer and shields C-steel from harmful ions.
- The morphology study is very important in case there is a difference between the amount of protection efficiency obtained from chemical and electrochemical techniques.
- The findings of the practical experiments match the theoretical calculations.

Author Contributions SE: conceptualization, investigation, methodology, resources, formal analysis, data curation, writing-original draft, writing-review & editing. KAS: conceptualization, investigation, methodology, resources, formal analysis, data curation, writing-original draft, writing-review & editing. AYE-E: conceptualization, investigation, formal analysis, writing original draft, writing-review & editing. EG: conceptualization, investigation, methodology, resources, formal analysis, data curation, writing-original draft, writing-review & editing. HN: conceptualization, investigation, methodology, resources, formal analysis, data curation, writing-original draft, writing-review & editing. All authors read and approved the final manuscript.

Funding Funding information is not available.

Data Availability All data generated or analyzed during this study are included in this published article.

Declarations

Conflict of interest The authors declare that they have no known competing financial interests or personal relationships that could have appeared to influence the work reported in this paper.

Ethical Approval Not applicable.

Consent for Publication All authors have read the article and given their consent for publication.

References

1. Hazzazi OA, Abdallah M, Gad EAM (2014) Inhibition effect of some cationic surfactants on the corrosion of carbon steel in sulphuric acid solutions: surface and structural properties. Int J Electrochem Sci 9:2237–2253
2. Hegazy MA, El-Tabei AS, Bedair AH, Sadeq MA (2012) An investigation of three novel nonionic surfactants as corrosion inhibitor for carbon steel in 0.5 M H2SO4. Corros Sci 54:219–230. https://doi.org/10.1016/j.corsci.2011.09.019
3. Adawy AI, Abbas MA, Zakaria K (2016) New Schiff base cationic surfactants as corrosion inhibitors for carbon steel in acidic medium: weight loss, electrochemical and SEM characterization techniques. Res Chem Intermed 42:3385–3411. https://doi.org/10.1007/s11164-015-2219-7
4. El-etre WIAY, El-Dougdoug ES, El-Din AN (2016) Synthesis and inhibition effect of two new fatty amido-cationic surfactants on carbon steel corrosion in 1 M HCl solution. J Basic Environ Sci 3:70–84

5. Tawfik SM (2015) Corrosion inhibition efficiency and adsorption behavior of N, N-dimethyl-4-(((1-methyl-2-phenyl-2, 3-dihydro-1H-pyrazol-4-yl) imino) methyl)-N-alkylbenzenaminium bromide surfactant at carbon steel/hydrochloric acid interface. J Mol Liq 207:185–194. https://doi.org/10.1016/j.molliq.2015.03.036
6. Abd El-Maksoud SA, Fouda AS, El-Habab AT et al (2021) Synthesis of some ethoxylated and sulfonated fatty alcohol surfactants and their inhibition actions for C-steel corrosion in 1 M HCl. J Bio Tribo Corros 7:44. https://doi.org/10.1007/s40735-021-00471-1
7. Alaoui K, Ouakki M, Abousalem AS et al (2020) Chemical, electrochemical, theoretical and surface morphology studies of triazepine carboxylate compounds as corrosion inhibitors for mild steel in hydrochloric acid medium. J Bio Tribo Corros 6:54. https://doi.org/10.1007/s40735-020-00352-z
8. Kavitha N, Kathiravan S, Jyothi S et al (2019) Adsorption and inhibitive properties of methanol extract of *Leucas aspera* leaves for the corrosion of mild steel in HCl medium. J Bio Tribo Corros 5:51. https://doi.org/10.1007/s40735-019-0244-6
9. Ma IAW, Ammar S, Kumar SSA et al (2022) A concise review on corrosion inhibitors: types, mechanisms and electrochemical evaluation studies. J Coat Technol Res 19:241–268. https://doi.org/10.1007/s11998-021-00547-0
10. Abbas MA, Bedair MA, El-Azabawy OE, Gad ES (2021) Anticorrosion Effect of Ethoxylate Sulfanilamide Compounds on Carbon Steel in 1 M Hydrochloric Acid: Electrochemical and Theoretical Studies. ACS Omega 6:15089–15102. https://doi.org/10.1021/acsomega.1c01274
11. Zucchi F, Trabanelli G, Brunoro G (1992) The influence of the chromium content on the inhibitive efficiency of some organic compounds. Corros Sci 33(7):1135–1139. https://doi.org/10.1016/0010-938X(92)90167-2
12. Abdallah M, Al-Tass HM, Jahdaly BAAL, Fouda AS (2016) Inhibition properties and adsorption behavior of 5-arylazothiazole derivatives on 1018 carbon steel in 0.5M H_2SO_4 solution. J Mol Liq 216:590–597. https://doi.org/10.1016/j.molliq.2016.01.077
13. Hegazy MA, El-Etre AY, El-Shafaie M, Berry KM (2016) Novel cationic surfactants for corrosion inhibition of carbon steel pipelines in oil and gas wells applications. J Mol Liq 214:347–356. https://doi.org/10.1016/j.molliq.2015.11.047
14. Negm NA, Elkholy YM, Zahoursan MK, Tawfik SM (2010) Corrosion inhibition efficiency and surface activity of benzothiazol-3-ium cationic Schiff base derivatives in hydrochloric acid. Corros Sci 52(10):3523–3536. https://doi.org/10.1016/j.corsci.2010.07.001
15. Idouhli R, N'Ait Ousidi A, Koumya Y, Abouelfida A, Benyaich A, Auhmani A, Itto MYA (2018) Electrochemical studies of monoterpenic thiosemicarbazones as corrosion inhibitor for steel in 1MHCl. Int J Corros. https://doi.org/10.1155/2018/9212705
16. Abdallah M et al (2016) Animal glue as green inhibitor for corrosion of aluminum and aluminum-silicon alloys in sodium hydroxide solutions. J Mol Liq 220:755–761
17. Zarrok H, Zarrouk A, Salghi R, Oudda H (2012) Gravimetric and quantum chemical studies of 1- [4-acetyl-2-(4 chlorophenyl)quinoxalin-1(4H)-yl]acetone as corrosion inhibitor for carbon steel in hydrochloric acid solution. J Chem Pharm Res 4:5056–5066
18. El Azzouzi M, Aouniti A, Tighadouin S, Elmsellem H, Radi S, Hammouti B, El Assyry A, Bentiss F, Zarrouk A (2016) Some hydrazine derivatives as corrosion inhibitors for mild steel in 1.0M HCl: weight loss, electrochemichal, SEM and theoretical studies. J Mol Liq 221:633–641. https://doi.org/10.1016/j.molliq.2016.06.007
19. Eddy NO, Odoemelam SA (2008) Norfloxacin and Sparfloxacin as corrosion inhibitors for zinc. Effect of concentrations and temperature. J Mater Sci 4(1):87–96
20. Fouda AS, Rashwan SM, Kamel MM, Ibrahim A (2015) Tenormin drug as save corrosion inhibitor for 304 stainless steel in hydrochloric acid solutions. Der Pharma Chemica 7(4):22–33
21. Abdel Hameed RS, Ismail EA, Abu-Nawwas AH, Hussin I, AL-Shafey, (2015) Expired voltaren drugs as corrosion inhibitor for aluminium in hydrochloric acid. Int J Electrochem Sci 10:2098–2109
22. Motawea MM, Gadow HS, Fouda AS (2016) Expired cidamex drug as corrosion inhibitor for aluminum in acidic solution. Glob J Res Eng (C) 16(1):7–18
23. Eid S (2021) Expired desloratidine drug as inhibitor for corrosion of carbon steel pipeline in hydrochloric acid solution. Int J Electrochem Sci 16:150852
24. Eddy NO, Ebenso EE, JIbok U (2010) Adsorption, synergistic inhibitive effect and quantum chemical studies of ampicillin (AMP) and halides for the corrosion of mild steel in H_2SO_4. J Appl Electrochem 40:445–456. https://doi.org/10.1007/s10800-009-0015-z
25. Geethamani P, Narmatha M, Dhanalakshmi R et al (2019) Corrosion inhibition and adsorption properties of mild steel in 1 M hydrochloric acid medium by expired ambroxol drug. J Bio Tribo Corros 5:16. https://doi.org/10.1007/s40735-018-0205-5
26. Ganapathi Sundaram R, Vengatesh G, Sundaravadivelu M (2017) Adsorption Behavior and Anticorrosion Capability of Antibiotic Drug *Nitroxoline* on Copper in Nitric Acid Medium. J Bio Tribo Corros 3:36. https://doi.org/10.1007/s40735-017-0097-9
27. Fajobi MA, Fayomi OSI, Akande IG et al (2019) Inhibitive performance of ibuprofen drug on mild steel in 0.5 M of H_2SO_4 acid. J Bio Tribo Corros 5:79. https://doi.org/10.1007/s40735-019-0271-3
28. Maduelosi NJ, Iroha NB (2021) Insight into the adsorption and inhibitive effect of spironolactone drug on C38 carbon steel corrosion in hydrochloric acid environment. J Bio Tribo Corros 7:6. https://doi.org/10.1007/s40735-020-00441-z
29. Attia MM, Soliman KA, Eid S, Mabrouk EM (2021) Experimental and theoretical study on some azo chromotropic acid dyes compounds as inhibitor for carbon steel corrosion in sulfuric acid. J Iran Chem Soc. https://doi.org/10.1007/s13738-021-02329-2
30. Frisch MJ, Trucks GW, Schlegel HB, Scuseria GE, Robb MA, Cheeseman JR, Scalmani G, Barone V, Mennucci B, Petersson GA, Nakatsuji H, Caricato M, Li X, Hratchian HP, Izmaylov AF, Bloino J, Zheng G, Sonnenberg JL, Hada M, Ehara M, Toyota K, Fukuda R, Hasegawa J, Ishida M, Nakajima T, Honda Y, Kitao O, Nakai H, Vreven T, Montgomery JA, Peralta JE, Ogliaro F, Bearpark M, Heyd JJ, Brothers E, Kudin KN, Staroverov VN, Kobayashi R, Normand J, Raghavachari K, Rendell A, Burant JC, Iyengar SS, Tomasi J, Cossi M, Rega N, Millam JM, Klene M, Knox JE, Cross JB, Bakken V, Adamo C, Jaramillo J, Gomperts R, Stratmann RE, Yazyev O, Austin AJ, Cammi R, Pomelli C, Ochterski JW, Martin RL, Morokuma K, Zakrzewski VG, Voth GA, Salvador P, Dannenberg JJ, Dapprich S, Daniels AD, Farkas JB, Foresman JV, Ortiz J, Cioslowski DJF (2009) Gaussian 09. Gaussian, Inc., Wallingford CT
31. M. Abdallah, E. M. Kamar, Salah Eid, A. Y. El-Etre, Animal glue as green inhibitor for corrosion of aluminum and aluminum-silicon alloys in sodium hydroxide solutions. Journal of Molecular Liquids, 220 (2016) 755–761. https://doi.org/10.1016/j.molliq.2016.04.062
32. Nady H, Elgendy A, Arafa WAA, Gad ES (2022) Insight into the inhibition performance of thiosemicarbazones as efficient inhibitors for copper in acidic environment, Combined experimental and computational investigations. Colloids Surf A: Physicochem Eng Asp 647:129208–129226. https://doi.org/10.1016/j.colsurfa.2022.129208
33. Ashassi-Sorkhabi H, Majidi MR, Seyyedi K (2004) Investigation of inhibition effect of some amino acids against steel corrosion

in HCl solution. Appl Surf Sci 225:176–185. https://doi.org/10.1016/j.apsusc.2003.10.00
34. Eid S, Hassan WMI (2015) Chemical and theoretical studies for corrosion inhibition of magnesium in hydrochloric acid by tween 80 surfactant. Int J Electrochem Sci 10:8017–8027
35. Abbas MA, Arafa EI, Gad ES, Bedair MA, El-Azabawy OE, Al-Shafey HI (2022) Performance assessment by experimental and theoretical approaches of newly synthetized benzyl amide derivatives as corrosion inhibitors for carbon steel in 1.0 M hydrochloric acid environment. Inorg Chem Commun 143:109758–109778. https://doi.org/10.1016/j.inoche.2022.109758
36. Bedair MA, Soliman SA, Bakr MF, Gad ES, Lgaz H, Chung I-M, Salama M, Alqahtany FZ (2020) Benzidine-based Schiff base compounds for employing as corrosion inhibitors for carbon steel in 1.0 M HCl aqueous media by chemical, electrochemical and computational methods. J Mol Liq 317:114015–114035. https://doi.org/10.1016/j.molliq.2020.114015
37. Ahmed AH, Sherif E-SM, Abdo HS, Gad ES (2021) Ethanedihydrazide as a corrosion inhibitor for iron in 3.5% NaCl solutions. ACS Omega 6:14525–14532. https://doi.org/10.1021/acsomega.1c01422
38. Alharthi NH, El-Hashemy MA, Derafa WM, Althobaiti IO, Altaleb HA (2022) Corrosion inhibition of mild steel by highly stable polydentate schiff base derived from 1,3- propanediamine in aqueous acidic solution. J Saudi Chem Soc 26:101501. https://doi.org/10.1016/j.jscs.2022.101501
39. Wagdy ED, Eid S, Zaher AA, El-Etre AY (2016) Inhibition of carbon steel corrosion in aqueous solutions using some fatty amidocationic surfactant. J Basic Environ Sci 3:55–64
40. Seyam DF, Tantawy AH, Eid S, EI-Etre AY (2021) Study of the inhibition effect of two novel synthesized amidoamine-based cationic surfactants on aluminum corrosion in 0.5 M HCl solution. J Surfact Deterg. https://doi.org/10.1002/jsde.12546
41. Li X, Deng S, Guannan Mu, Hui Fu, Yang F (2008) Inhibition effect of nonionic surfactant on the corrosion of cold rolled steel in hydrochloric acid. Corros Sci 50(2):420–430. https://doi.org/10.1016/j.corsci.2007.08.014
42. Haque J, Srivastava V, Quraishi MA, Chauhan DS, Lgaz H, Chung IM (2020) Polar group substituted imidazolium zwitterions as eco-friendly corrosion inhibitors for mild steel in acid solution. Corros Sci 172:108665. https://doi.org/10.1016/j.corsci.2020.108665
43. Zhang W, Ma Y, Chen L, Wang L-J, Wu Y-C, Li H-J (2020) Aloe polysaccharide as an eco-friendly corrosion inhibitor for mild steel in simulated acidic oilfield water: experimental and theoretical approaches. J Mol Liq 307:112950. https://doi.org/10.1016/j.molliq.2020.112950
44. Kosari A, Moayed MH, Davoodi A, Parvizi R, Momeni M, Eshghi H, Moradi H (2014) Electrochemical and quantum chemical assessment of two organic compounds from pyridine derivatives as corrosion inhibitors for mild steel in HCl solution under stagnant condition and hydrodynamic flow. Corros Sci 78:138–150. https://doi.org/10.1016/j.corsci.2013.09.009
45. Dagdag O, Hsissou R, Berisha A, Erramli H, Hamed O, Jodeh S, El Harfi A (2019) Polymeric-based epoxy cured with a polyaminoamide as an anticorrosive coating for aluminum 2024–T3 surface: experimental studies supported by computational modeling. J Bio-Tribo-Corros 5:58. https://doi.org/10.1007/s40735-019-0251-7
46. Hsissou R, Abbout S, Berisha A, Berradi M, Assouag M, Hajjaji N, Elharfi A (2019) Experimental, DFT and molecular dynamics simulation on the inhibition performance of the DGDCBA epoxy polymer against the corrosion of the E24 carbon steel in 10 M HCl solution. J Mol Struct 1182:340. https://doi.org/10.1016/j.molstruc.2018.12.030